

Expected properties of radio pulses from lunar EeV neutrino showers

A. R. Beresnyak*

Puschino Radio Astronomy Observatory, Puschino, Moscow region 142290, Russia

December 24, 2018

Abstract

We present results of the simulation of the intensity distribution of radio pulses from the Moon due to interaction of EeV neutrinos with lunar regolith. The radiation mechanism is of coherent Čerenkov radiation of the negative charge excess in the shower, known as Askar'yan effect. Several realistic observational setups with ground radio telescopes are considered. Effective detector volume is calculated using maximum-knowledge Monte Carlo code, and the possibilities to set limits on the diffuse neutrino flux are discussed.

1 Introduction

Due to the lack of atmosphere on the Moon, its surface has been proposed as a target for detection of cosmic rays by mounting detectors on the Moon as early as in the original Askar'yan's papers [1]. Using the whole visible lunar surface with its huge effective volume by monitoring the Moon with ground based radiotelescope has been first proposed in [2]. Large effective volume presumed detection of particles with extremely low fluxes, while the distance from the observer limits to the very energetic events. Using Askar'yan's effect for detection of neutrinos of cosmic rays is considered advantageous, since shower coherent radio emission grows roughly as a square of initial particle energy, and with this consideration in mind it had hoped to overcome the steep decline in flux expected from known CR spectrum. However the first rough estimates, [2], has been shown to be too optimistic. This is due to the particular target geometry: neutrinos at EeV energies are expected to have rather high cross-section, and the detectable events will be only those crossing the edge of the Moon, and the fact that Čerenkov angle is complimentary to the full internal reflection angle.

Up to now, there has been several attempts to detect ultrashort radio pulses from the Moon [3,4] none of which shown any signs of such pulses. However, these observations, combined with the detailed modeling of the emission will allow to reject particular models of EeV neutrino spectrum.

Particles with energies around 10^{20} eV and higher became one of the major interest in the field of CR science since the formulation of the GZK paradox [5,6]. That is, starting with $5 \cdot 10^{19}$ eV particles loose energy on the pion production interacting with CMB on scales of around 10Mpc, while the our Galaxy's or stochastic intergalactic magnetic fields is not high enough to sufficiently curve them. So we expect to see the sources of such particles which should be relatively nearby,

*E-mail: beres@prao.psn.ru

but up to now, with around a hundred cosmic ray events detected near the GZK energy, they seem to be distributed rather uniform on the sky.

The expected sources of neutrinos with GZK energies, ranging from certain, such as GZK cosmic rays, to possible, such as AGNs and exotic – topological defects or massive relic particles, predict neutrino flux somewhat or of the order of magnitude higher than CR flux. Beyond GZK limit this difference might be even bigger, so it is no wonder that detection of extra high energy neutrinos received a considerable attention lately [3,4,8,10,11,14,17-19].

The observation of the Moon with ground radio telescopes could either detect EeV neutrinos or put a limit on their flux. This paper studies various aspects of such observations and tries to find the most favorable setups.

2 Coherent Čerenkov radiation

Well known Frank-Tamm formula for particle Čerenkov losses in dense media, usually found in textbooks is not applicable in our case. This formula addresses the case of infinite track length, hence, inevitably, near-field region. However, the formula for finite track, in the Fraunhofer limit, has indeed been known for a long time [7]:

$$\frac{d^2P}{d\omega d\Omega} = \frac{ne^2\omega^2L^2}{4\pi^2c^3} \sin^2 \theta \frac{\sin^2 X}{X^2}, \quad (1)$$

Here P is the *total energy* radiated in a given solid angle in a given frequency range, *already summed* from positive and negative frequency parts, n is the refraction index, L is the track length, θ_c is the Čerenkov angle, X is the phase equaled to $n\omega L(\cos \theta_c - \cos \theta)$ ¹. The most prominent difference from the infinite track formula is in the frequency dependence with flux growing like the frequency squared, rather than the frequency in the first power.

Maxwell's equation for the infinite space filled with dielectric with permittivity of ϵ , and permeability of unity, will give the following solution for the Fourier component of the electric field

$$\vec{E}(\omega, \vec{x}) = \frac{i\omega}{c^2} \int dt' d^3\vec{x}' e^{i\omega t' + ik|\vec{x} - \vec{x}'|} \frac{\vec{J}_\perp}{|\vec{x} - \vec{x}'|}. \quad (2)$$

Here we defined Fourier component of \vec{E} as

$$\vec{E}(\omega) = \int_{-\infty}^{\infty} \vec{E}(t) e^{i\omega t} dt. \quad (3)$$

In this normalization the radiated energy, similar to one presented in (1), that is having no negative frequency part will be

$$\frac{d^2P}{d\omega d\Omega} = \frac{cn}{4\pi^2} |RE(\omega)|^2. \quad (4)$$

From the first glance (2) does not contain any traces of the properties of the media. However, k here is not a variable, it is determined by the Čerenkov resonance condition $k = n\omega/c$. This expression can be reduced further by using Fraunhofer, or far field limit, that is, approximating $|\vec{x} - \vec{x}'|$ to the linear order and assuming a particular charge current distribution.

¹CGS units are used unless otherwise noted.

Since particles in a shower move mostly along one particular axis, the current density could be decently approximated by

$$\vec{J}_\perp(\vec{x}, t) = Q(z)\hat{n}_\perp c \sin \theta \delta^3(\vec{x} - n_z ct). \quad (5)$$

And the electric field, from (2),

$$\vec{E}(\omega, \vec{x}) = \frac{i\omega}{c^2} \sin \theta \frac{e^{ikR}}{R} n_\perp \int Q(z') e^{ipz'} dz', \quad (6)$$

where $p = (1 - n \cos \theta)\omega/c$. The angular dependence of the electric field amplitude near Čerenkov angle may be seen as a Fourier transform of the longitudinal charge distribution. From here it is easy to reproduce finite track Frank-Tamm formula, (1).

This so called one-dimensional approximation works surprisingly well in describing maximum intensity at low frequencies and angular dependence [8]. But, rather obviously, it fails to describe decoherence that comes from the transverse spread of the shower.

There has been several independent Monte-Carlo simulations of showers and their Čerenkov electric field [9,10,11]. The results are in pretty good agreement, concerning integral quantities such as the total projected (e-p) tracklength, L , which determines the field at the Čerenkov angle at low frequencies.

$$R|E(\omega, \theta = \theta_C)| = \frac{e\omega L \sin \theta}{c^2} \quad (7)$$

The tracklength has been shown to scale linearly with the energy of the showers, or with the electromagnetic energy in the hadronic showers. The accelerator observation of the effect [12] does also comply reasonably well with this simulations.

The first estimates of the decoherence from the transverse spread of the shower were done as early as in one of the pioneering Askaryan papers [1]. Indeed, this issue is important for choosing the best observation frequency and for estimates of maximum coherent flux.

In the present paper we adhere to the particular parametrization for the electric field of one of these simulations, [8], assuming that tracklength, decoherence frequency and the angular width of the Čerenkov cone scale with radiation length.

The decoherence is described by the phenomenological form-factor fitting electric field intensity at the Čerenkov angle, [8]

$$F(\nu) = \frac{1}{1 + (\nu/\nu_0)^{1.44}}, \quad (8)$$

We have to note, however, that different shower MC's do not agree very well at frequencies higher than decoherence frequency, which is around 2.5GHz for regolith.

3 Showers

As we see from (6) the longitudinal profile of the shower determines the angular width and the form of the Čerenkov electric field peak. Showers with energies higher than 1 TeV but less than 1 PeV do not fluctuate much and have profiles close to gaussian, with longitudinal spread growing slowly with energy as $\sqrt{2/3 \log(E_0/E)}$ [13]. Starting with energies around 10 PeV, electromagnetic showers are affected by Landau Pomeranchuk Migdal effect [15]. Due to suppressed interaction at high energies the shower looks as a combination of several subshowers, with normal length, that

is of several radiation lengths. The number of these subshowers are usually not enough to add up to the good averaged gaussian profile, so LPM showers fluctuate a lot. In fact, each of them has the individual form. However the Fourier transform of such a sparse showers have some general features. Namely, there are two characteristic lengths, one of the total length of the shower, and the other is 7-9 radiation lengths, the typical length of a non-LPM shower at these energies. So, the Fourier transform have an envelope inside of which there is a typical interference pattern, and the total shower length determine the width of an individual peaks.

Neutrino or antineutrino interacting with nucleon's quark by charged current (W^\pm) gives the corresponding charged lepton and changes the flavour of the quark. The energy fraction transferred to the quark y , and the fraction of the nucleon's momentum carried by the struck quark x are called Bjorken variables. The charged lepton, say, the muon, then initiate electromagnetic shower of energy $(1-y)E_\nu$, and the quark initiate hadronic shower of energy yE_ν . Due to the high multiplicity of the collisions governed by strong force high initial energy in hadronic shower got divided pretty quickly, thus mitigating the LPM effect. It has been shown than some hadronic showers of energy as high as 100EeV show little or no LPM elongation, while the others are lengthening only by several tenths percent [18]. So, the charge current interacting neutrino produces two distinctly different showers, the Čerenkov electric field being the sum of that of each of them. The neutral current (Z) interactions got neutrino scattered, and produces only hadronic shower of energy of yE_ν .

The deep inelastic scattering (DIS) cross sections for the energies in question is determined mainly by the behavior of the distribution function of the sea quarks at low values of x , such as $x \approx M_W^2/2ME_\nu y$ which is $3 \cdot 10^{-8}/y$ at $E_\nu = 10^{20}$ eV. The distribution function at these x has not been measured directly, however it could be extrapolated from lower values of x by the power law with index of around -1.3 [19]. We assumed $xq_s(x) \approx x^{-0.33}$. This parametrization gives an semianalytic expression for the $d\sigma/dy$ dependence we are interested in. For example, for muon neutrino the differential cross section is proportional to $(3 + 2(1-y)^2)y^{0.67}$ for charged current and $(1 + (1-y)^2)y^{0.67}$ for neutral current, mean values of y being 0.2 and 0.19 correspondingly.

The total νN CC and NC cross sections were taken from the parametrization in [19], σ_{NC} being a 0.42 fraction of σ_{CC} .

4 Time dependence

Determining the time dependence of the real Čerenkov pulse might be a tricky matter. Not all $E(\omega)$ which seem close or give close fits to the Monte Carlo would give physically reasonable time dependence. As has been noticed in [14] analytic structure of $E(\omega)$ in the complex plane play a major role in the form of $E(t)$, even though the $E(\omega)$ itself is determined only in the real axis by a numerical fit.

Even though early papers on Askaryan effect suggested using full-bandwidth ionospheric-delay compensated radio observations which will maximize signal-to-noise ratio and make use of the unique Čerenkov pulse shape [2], it would probably be the way only future dedicated instruments will work. All experiments up to date used a bandwidth limited, maximum flux triggered setup.

A pulse whose duration smaller than an inverse bandwidth, passed through a filter, would give a maximum flux density, a flux per unit frequency, which is roughly equal to the total energy received in this bandwidth. This relation is routinely used wherever there is a need to relate time and frequency dependent fluxes, but it should be remembered that it is not exact. The exact correspondence between these quantities depends on the particular frequency characteristic of the

filter. It would be ideal that any detector be tried and calibrated with the pulse whose form is close to the real one.

5 Geometry and refraction

The solid angle of the part of the ray caught by the telescope is much smaller than the typical refracted Čerenkov cone, so we can use ray optics. According to the effect mentioned in the introduction there should be strong damping of the outgoing radiation, however, as it was found, the transmissivity at the regolith-vacuum interface is not much to blame. As it follows from the geometry of the most detectable events, the E vector will lay close to the plane of refraction, however the T_{\parallel} transmission coefficient, being zero at total reflection angle, rises sharply to 1 in a few degrees.

It is the solid angle stretching near zero angles that does the most effect. Indeed, the solid angle before and after refraction will have the ratio of

$$\frac{d\Omega}{d\Omega'} = \frac{\sin \beta}{n^2 \sin \alpha},$$

where β is an angle between the plane of the surface of the Moon and the outgoing ray, and α is the same angle for incoming ray. This coefficient scales like β at small angles, as well as T_{\parallel} does, however it is much smaller than T_{\parallel} for the angles of a few degrees – the ones we are interested in. As an example in Figure 1 we showed the full exact damping coefficient which is the product of the above ratio to the T_{\parallel} , plotted versus $r = 1 - \cos \beta$. r may be thought of as a relative distance of the event from lunar limb, $r = 0$ correspond to the limb, $r = 1$ to the center. Both transmissivity and solid angle stretching is proportional to β at small β , however for transmissivity this law fails already at a few degrees.

It is also interesting to calculate which part of the incoming particles full 4π solid angle will give radiation coming out of the Moon, though not necessarily detectable, in the assumption that all radiation is concentrated in the cone with typical angle estimated in section 2. This “effective” solid angle is shown on figure 2. It happened, that those neutrinos that have positive entrance angles, that is those, that hit the visible hemisphere, give important income to this total angle, especially at low frequencies and low β ’s.

As we see from Figures 1 and 2 both the effective solid angle and the intensity damped by more than order of magnitude, which undermines previous optimistic estimates [2] and brings close attention to the detailed modeling of the transmissivity properties of the lunar-vacuum interface. In the next section we describe such a modeling.

6 Monte Carlo

We modeled a 64 meter telescope with standard circular aperture, pointed at some point between lunar center and the limb, making observations at some frequency ν with a bandwidth of 100 MHz, set up so to trigger events which have a total flux density higher than a certain threshold.

For each prospective CC or NC event we generated its lunar coordinates, depth at which interaction took place, two angles of the incoming neutrino, Bjorken y , calculated the radio flux taking into account LPM by parametrizations from [17,18] and polarization position angle. We used exact formulae for transmissivity of two different polarizations, adopted absorption length of 15 m(1 GHz/ ν). We assumed that regolith or some other material with similar properties cover the

Figure 1: The full damping at the regolith-vacuum interface, versus relative distance from the limb

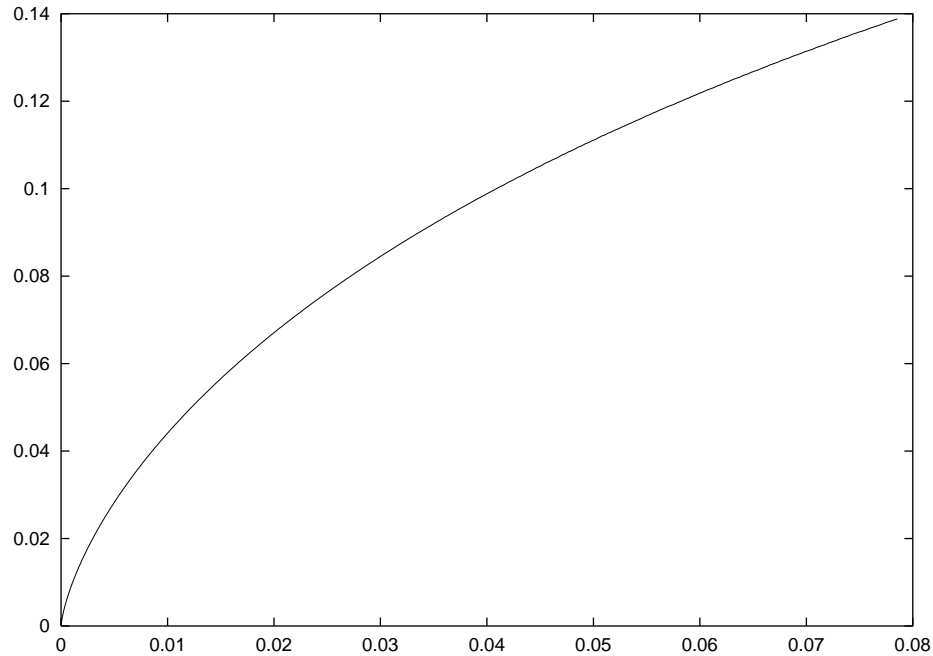


Figure 2: The effective solid angle versus output angle, in the assumption that radiation coming from Čerenkov cone is always observed

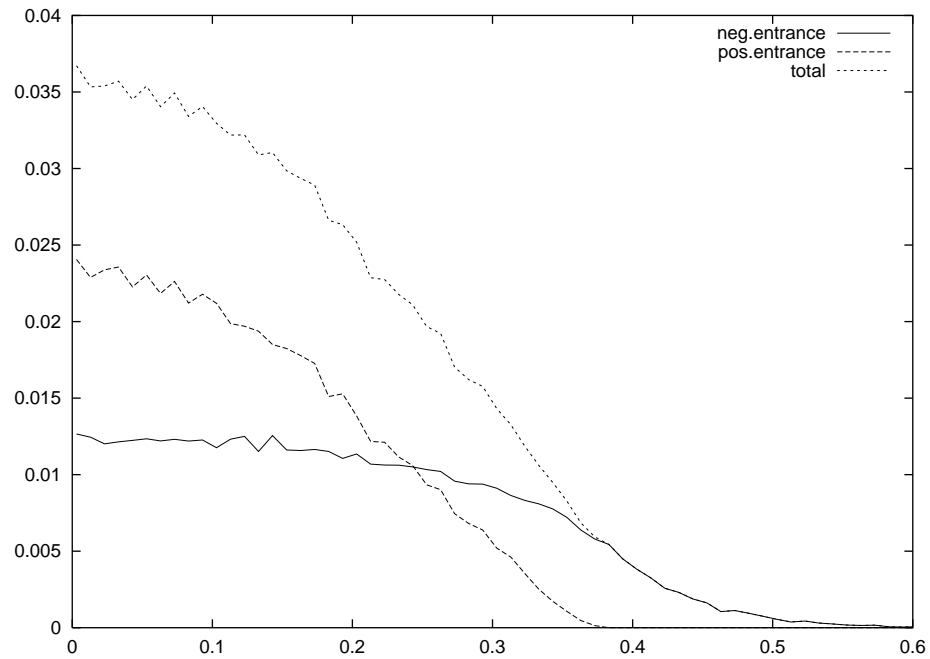
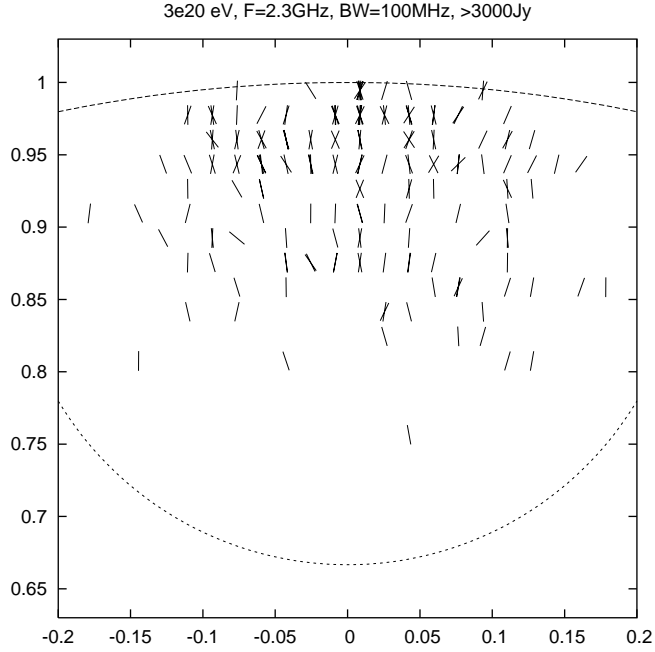


Figure 3: Some events as seen on the Moon’s face. Upper circle is the Moon’s limb, lower shows the telescope beam. Polarization is shown with electric field vectors.



Moon with a layer of at least 30 meters deep, which somewhat increased effective volume at very high energies. We adopted the lunar surface roughness model with rms slope of 6° at the length scales we are interested in. The angular dependence of the shower radio flux, and the angular dependence of the sensitivity of the telescope were both taken into account.

Several events with their polarizations were drawn on Figure 3. The frequency of observation was 2.3 GHz and the flux density limit 3000 Jy. The telescope was aimed 13.5' from the lunar center. As we see, most of the events are concentrated close to the rim, and this behavior becomes more prominent with higher energies, since the neutrino interaction length shortens. As it comes from a theory, all events are fully linearly polarized, and polarization tends to align along radius-vector to the lunar center.

Neutrinos with positive entrance angles give almost no contribution at low energies, $< 10^{20}$ eV, however their relative contribution grows as cross-section grows, at 10^{23} eV contributing about the half of all trigger events.

Even though the mean value of y is around 0.2, that is most of the time most of the energy goes to either electromagnetic shower or neutrino, in this geometry electromagnetic showers happen to be relatively unimportant for radio detection. They contribute to trigger significantly only close to the edge of detection, which is around 10^{20} eV for 2.3 GHz and a bandwidth of 100 MHz. The number of triggers came purely from EM showers do not grow much with energy.

The effective detector volume for the same frequency and a limit of 3000 Jy as dependent on primary particle energy is shown on Figure 4.

Figure 5 shows the detector volume for different neutrino energies as dependent from radio telescope orientation. Maximum, as expected, is achieved close to the lunar rim.

Figure 4:

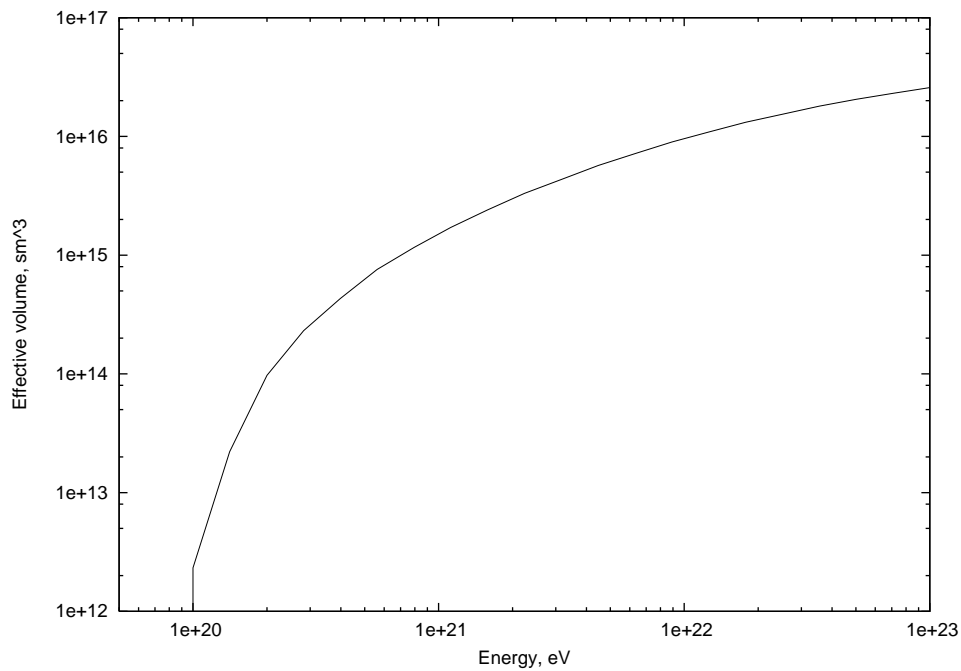


Figure 5:

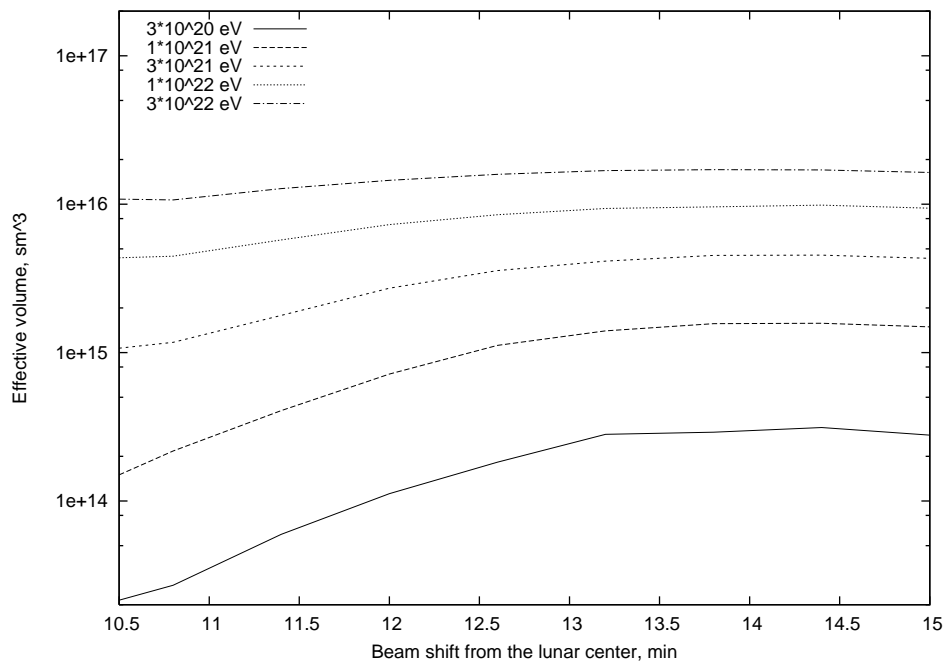
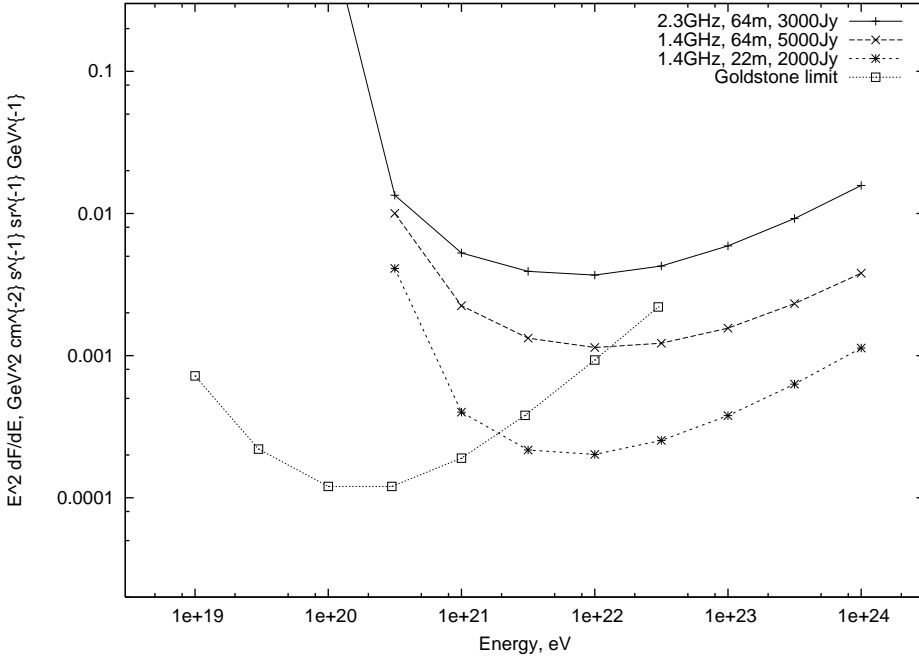


Figure 6:



7 Diffuse neutrino flux limits

Having neutrino cross-section, the observational time, and the effective volume deduced in a previous section it is straightforward to estimate a diffuse neutrino flux at a given energy, having several events detected, or put an upper limit on this flux if there were no detection.

However, it must be stressed, that the fact of no-detection, logically, allows us to reject only one *particular* model spectrum of the cosmic neutrinos. It allows not the upper limits on a real differential flux curve $E^2 dF/dE$ at any given energy. Indeed, the differential flux might have a thin but high fluke constituting only a small amount of an integrated flux, which surely will not be detected.

Hence, the correct statement must be that we exclude the possibility of a neutrino flux higher than F_ν with energies of neutrinos being between E_{\min} and E_{\max} with certain confidence level. Once the fact of no-detection is used it could not be reused to make any other such statements.

Figure 6 shows some constraints which came from 30 hours of observations for several observational setups. Solid and dashed lines correspond to the 64m telescope aimed 13.5' from lunar center, observations being at central frequencies of 2.3 and 1.4 GHz with bandwidth of 100 MHz and a flux limit of 3000 and 5000 Jy correspondingly. Crisscrossed points correspond to the observations with several 22m dishes aimed directly at lunar center, frequency is 1.4 GHz, BW is 100 MHz, number of dishes and the coincident scheme allowing a flux limit as low as 2000 Jy. The datapoints here should be understood in a manner described above, that we can exclude a model represented by two adjacent points with lines between them, and a zero differential flux at all other energies. No exclusion of a model curve as a whole is possible. As a comparison, we have shown limits obtained in [4], using about the same flux limit and the 30 hours of observations.

8 Acknowledgments

I am grateful to R. D. Dagkesamanskii and I. M. Zheleznykh for fruitful discussion and suggestions. This work was partially supported by Russian Foundation of Base Research grant N 02-02-17229.

9 References

1. Askaryan G.A., 1962, JETP 14, 441; Askaryan G.A., 1965, JETP 21, 658
2. Dagkesamanskii R.D., Zheleznykh I.M., JETP Lett, 50, 233 (1989)
3. Hankins T.H., Ekers R.D., O'Sullivan J.D., 1996, MNRAS, 283, 1027.
4. Gorham P.W., et al, 2001, Proc. RADHEP-2000, p.177.
5. Greisen K., Phys. Rev. Lett. **16**, 748 (1966)
6. Zatsepin G.T., Kuzmin V.A., Pisma Zh. Eksp. Teor. Fiz. **4**, 114 (1966)
7. Tamm I.E., J. Phys. (Moscow) 1, 439 (1939).
8. Alvarez-Muñiz J.; Vázquez R. A.; Zas E., Phys. Rev. **D**,**62**,063001 (2000)
9. Zas E., Halzen F., and Stanev T., Phys. Rev. **D**, **45**, 362 (1992)
10. Razzaque S., et al Phys. Rev. **D**, **65**, 103002, (2002)
11. Provorov A. L. and Zheleznykh I. M., Astropart. Phys. 4, 55 (1995)
12. Saltzberg D., Gorham P.W., et al., 2001, Phys. Rev. Lett., **86**, 13, 2802.
13. Rossi B., Greisen K., Rev. of Mod. Phys. **13**, No.4, 240-309; Rossi B., High Energy Particles (Prentice Hall, New York, 1952)
14. Buniy R.V., Ralston J.P., Phys.Rev. **D** **65**, 016003 (2002)
15. L. Landau and I. Pomeranchuk, *Dokl. Akad. Nauk SSSR* **92** (1953) 535; **92** (1935) 735; A.B. Migdal, Phys. Rev. **103** (1956) 1811; Sov. Phys. JETP **5** (1957) 527.
16. Butkevich A.V., et al, Z. Phys. C, **39**, 241-250 (1988)
17. J. Alvarez-Muñiz, E. Zas, Phys.Lett. B411 (1997) 218-224
18. J. Alvarez-Muñiz, E. Zas, Phys.Lett. B434 (1998) 396-406
19. Gandhi R., et al, Phys.Rev. D **58** (1998) 093009